Geological mapping by the use of multispectral and multitemporal satellite images, compared with GIS geological data. Case studies from Macedonia area, Northern Greece.

Dimitrios Oikonomidis, Antonios Mouratidis, Theodore Astaras and Mihail Niarhos
Laboratory of Remote Sensing and GIS Applications, Geology Dept. Aristotle University of Thessaloniki, Macedonia, Greece.
Lecturer Dimitrios Oikonomidis: oikonomi@geo.auth.gr

esa space for europe

1. Location and physical background of the study areas
Two study areas have been selected (Figure 1):
1) Kassandra peninsula, in Halkidiki Prefecture, Macedonia Province, Northern Greece
2) Thassos island, in Kavala Prefecture, Macedonia Province, Northern Greece.

Figure 1. Location of the study areas: Kassandra peninsula (red rectangle, lower) and Thassos island (black rectangle, higher)

2. Materials-Methodology
The following data were used:
- Geological maps of Kassandra peninsula and Thassos island (source: IGME/Institute of Geological and Mineral Exploration)
- Landsat-7/ETM+ satellite image, covering both study areas, acquisition date: 11 January 2001 (http://image2000.jrc.ec.europa.eu)
- TERRA/ASTER satellite images: 2 images for covering Kassandra peninsula, acquisition date: 10 August 2004 and 2 images for covering Thassos island, acquisition date: 13 July 2008.

Image processing software: ENVI 4.6.
GIS software: ArcGIS 9.3.
Lithological units and faults were digitized from the maps of IGME. After that, geological maps (simplified lithology and faults) and rose diagrammes were constructed (Figures 2-3). Then, certain digital image processing was applied to the satellite images, so that lithological units and photo-lineaments could be extracted. Lithological units and lineaments' maps were also produced. Finally, rose-diagrammes were constructed for comparing tectonic data from geological maps and lineaments derived from satellite images.
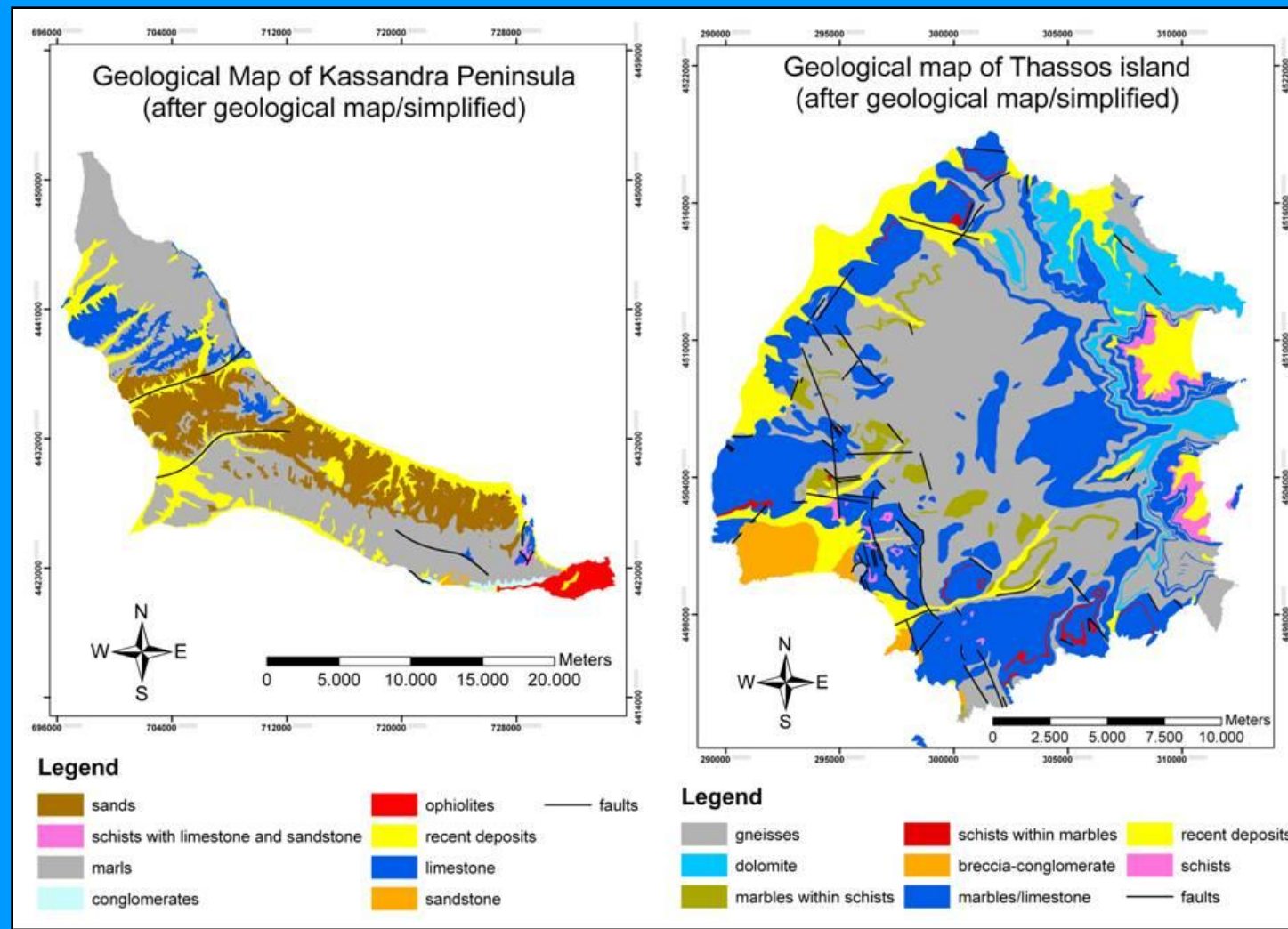

Figure 2. Geological maps (lithology and faults) of the Kassandra peninsula (2a/left) and Thassos island (2b/right), derived from geological map of IGME (simplified by Oikonomidis et al. 2009).
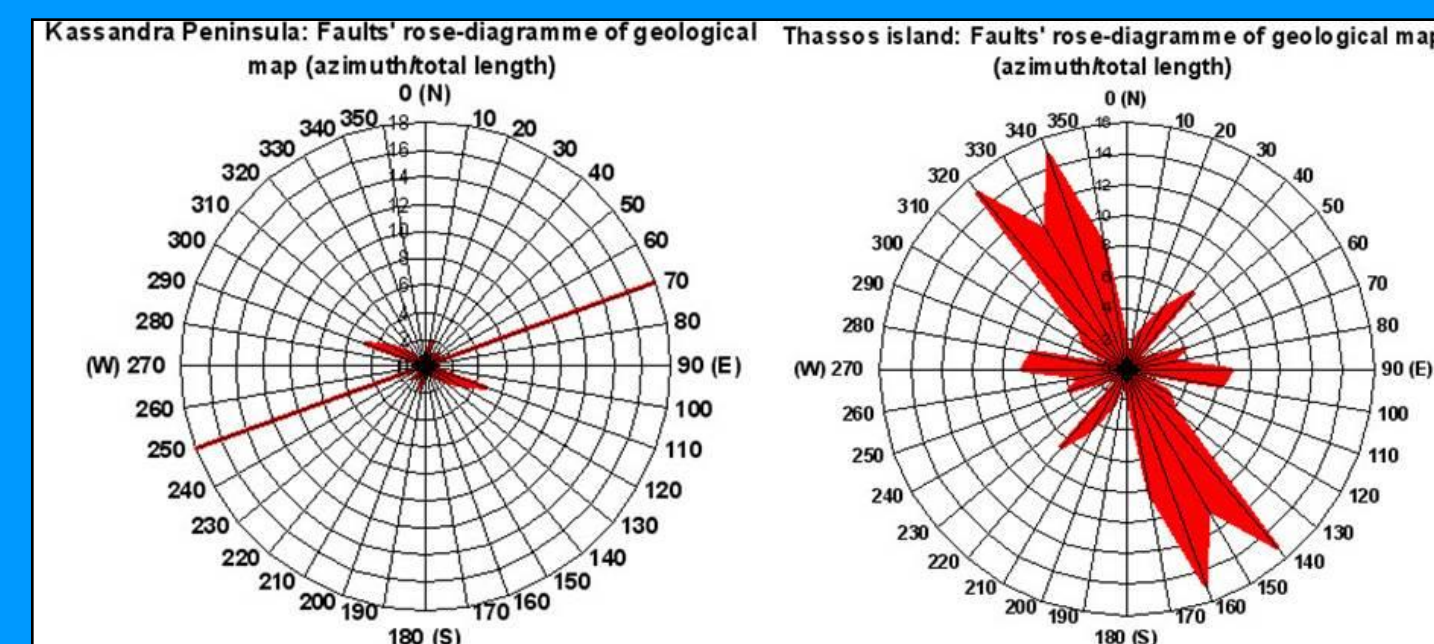

Figure 3. Faults' rose-diagrammes (azimuth/total length per class): Kassandra peninsula (3a/left) and Thassos island (3b/right).

3. Landsat-7/ETM+ image processing
Landsat-7 ETM+ image contains both multispectral and panchromatic bands with different spatial resolutions (30m and 15m). For this reason, an image sharpening methodology (else called merging or fusion) had to be applied, so that all the bands would have the same pixel size and could be processed easier. There are numerous methodologies for this, such as Principal Components Analysis/PCA sharpening, IHS (or HSV) sharpening and Color Normalized (Brovey) sharpening. Among them, the PCA sharpening was chosen because by this technique we can have all 6 multispectral bands (except the thermal one) sharpened at once and not only 3 at a time.

In the PCA sharpening, a principal components transformation is performed on the multispectral data. The PC band 1 is replaced with the high-resolution band (PAN in our case), which is scaled to match the PC band 1, so that no distortion on the spectral information occurs. Then , an inverse transform is performed. The multispectral data is automatically resampled to the high resolution pixel, using a nearest neighbour, bilinear or cubic convolution technique (ENVI User's Guide, 2005).

3.1 Landsat-7/ETM+ image processing/lithological mapping
The second step was to produce a Natural Difference Vegetation Index/NDVI image which has the form NIR-R/NIR+R. In the case of a ETM+ image, the formula becomes 4-3/4+3. This was necessary to be done to extract areas with dense vegetation (bright pixels).

Several image processing techniques, from past-published papers, including HSV and PCA transformation, band ratios, filtering and simple False Colour Composites/FCCs were applied on the Landsat image for extracting lithological boundaries, but the results were not satisfactory.

The best results occurred when a 742:RGB FCC was converted to IHS or HSV (Hue, Saturation Value) colour space and from that, back to RGB. Furthermore, a linear 2% radiometric enhancement was applied on the above image. As a result, an image occurred which proved to be more suitable for lithological mapping, compared to others, for our study areas (Figures 4a and 4b). A digitization of lithological boundaries on this image, produced the maps of Figures 5a and 5b.
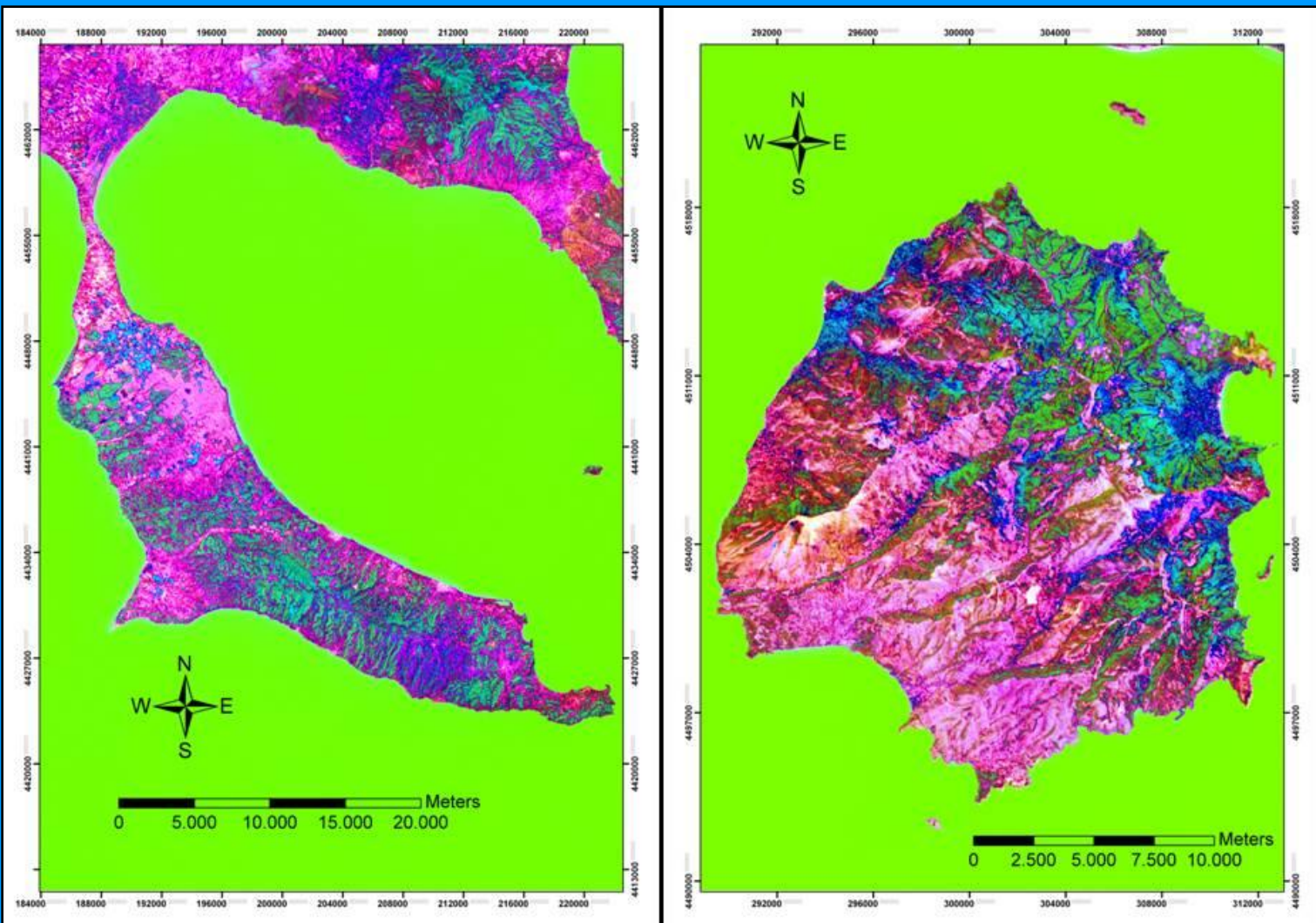

Figure 4. 742 HSV/RGB Landsat images: Kassandra peninsula (4a/left) and Thassos island (4b/right).
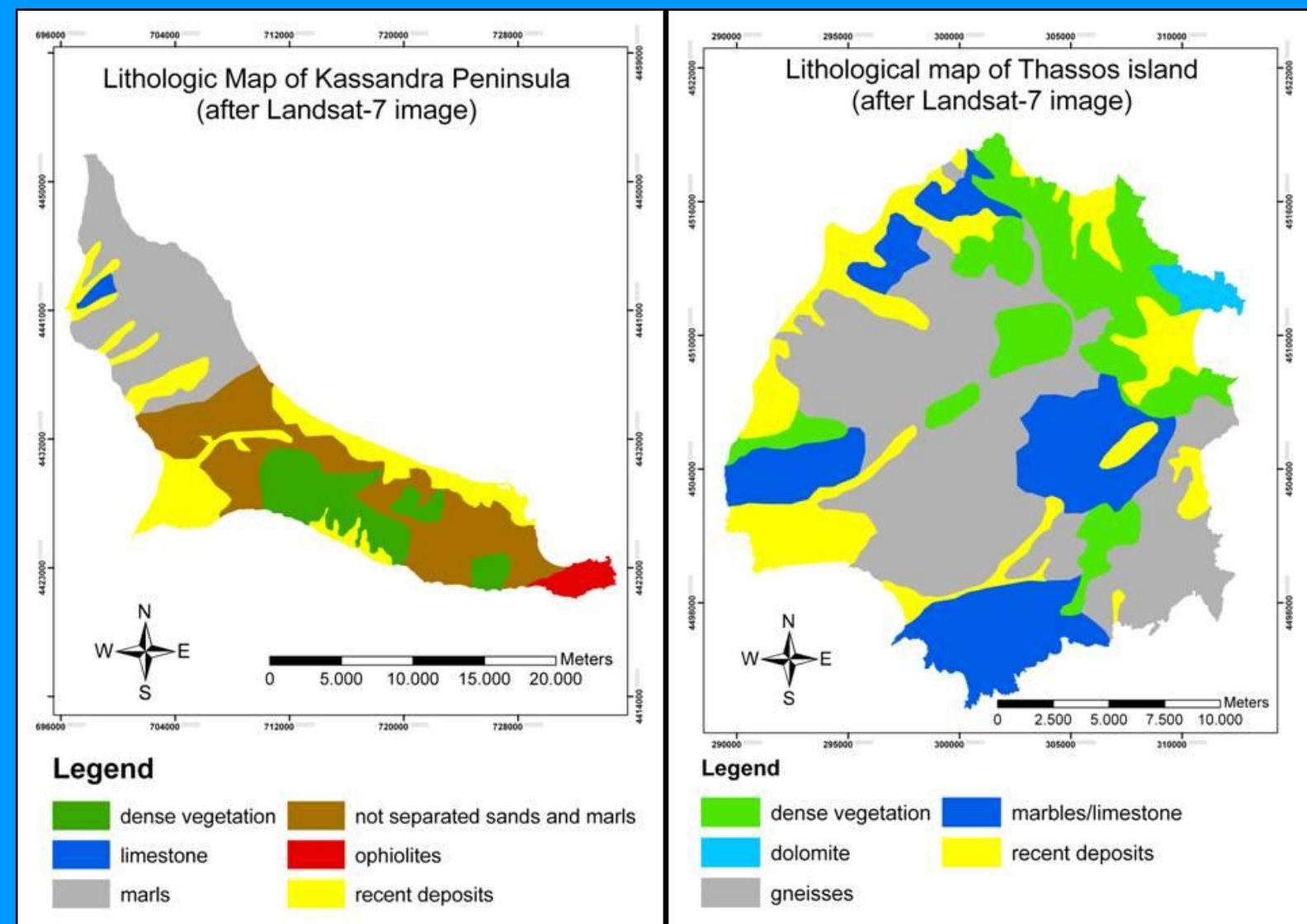

Figure 5. Lithological maps derived from the Landsat-7 image of Figure 4: Kassandra peninsula (5a/left), Thassos island (5b/right).

3.2 Landsat-7/ETM+ image processing/lineaments mapping
Concerning lineaments, the most suitable methodology applied on the Landsat image, proved to be the 5/3,5/1,7/3:RGB FCC image (Raharimahefa and Kusky, 2009). An equalization enhancement was applied on the above image for improvement. After the digitization of lineaments on this image, the images-maps of Figures 6a and 6b were created. The rose-diagrammes of the lineaments drawn, are shown on Figure 7.
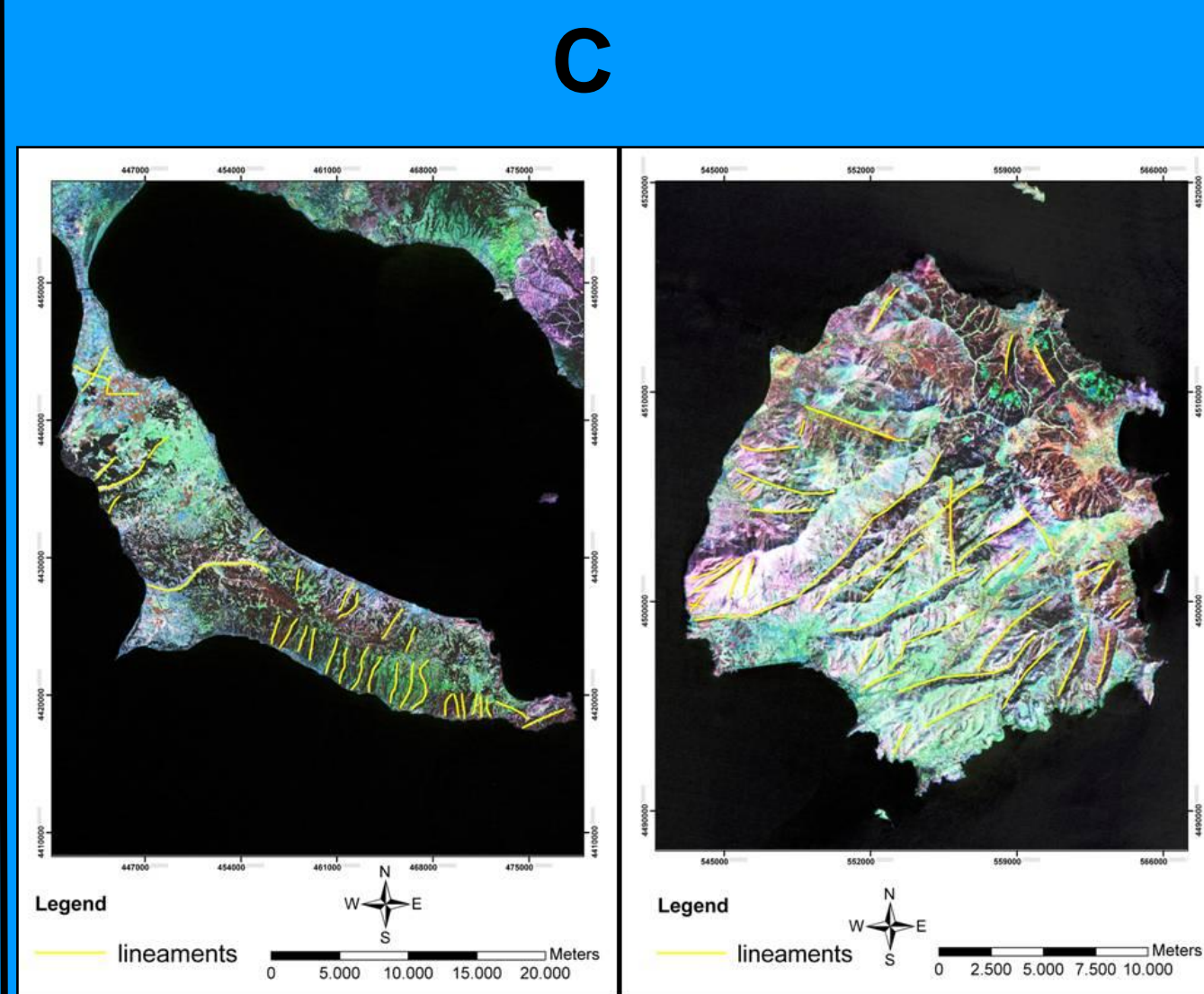

Figure 6. Lineaments delineated form 5/3,5/1,7/3:RGB Landsat images: Kassandra peninsula (6a/left) and Thassos island (6b/right).
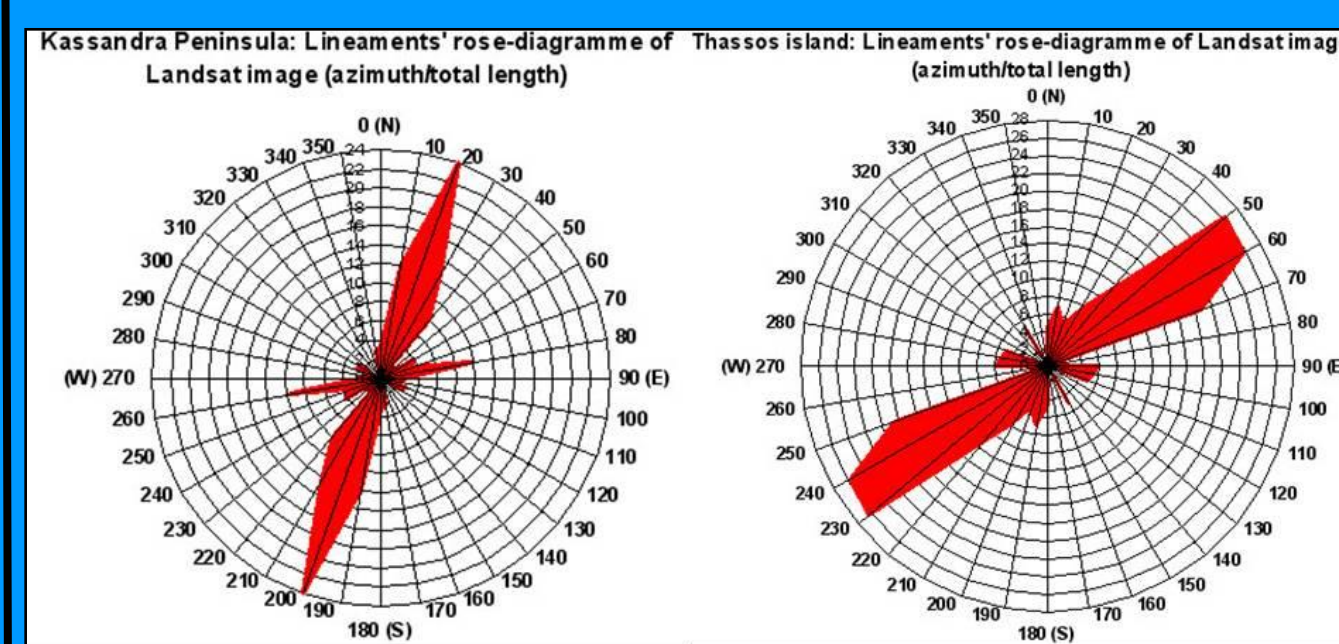

Figure 7. Lineaments' rose-diagrammes (azimuth/total length per class): Kassandra peninsula (7a/left) and Thassos island (7b/right), as derived from Landsat image.

4. TERRA/ASTER image processing
In the case of ASTER images, we had to order 2 images for each study area, since they were on the boundary of two successive ASTER images. Therefore, a mosaicking procedure had to take place, in order to be able to see our study areas in a whole, for each band separately. After that, we performed layer stacking, so that we could have in 2 files, the VNIR and SWIR bands.

As in the case of the Landsat image, an image sharpening methodology had to be applied, so that all the bands would have the same pixel size and could be processed easier. Again, the PCA sharpening methodology was used for VNIR and SWIR bands and as a result, a new file with 9 bands was created, having 15 m spatial resolution.

In the case of Thassos island, the only available cloud-free images were those of 13 July 2008, but due to a malfunction of the SWIR detectors, images are not recorded at the SWIR spectrum since April 2008, therefore the ASTER images of Thassos were practically not utilized.

4.1 TERRA/ASTER image processing/lithological mapping
The second step was to produce a Natural Difference Vegetation Index/NDVI image. In the case of a TERRA/ASTER image, the formula becomes 3-2/3+2.

Several image processing techniques, from past-published papers, including PCA and Minimum Noise Fraction/MNF FCCs, Indices FCCs, Spectral Angle Mapper/SAM, band ratios and simple FCCs were applied on the ASTER image for extracting lithological boundaries, but the results were not satisfactory.

The best results occurred when a PCA1,7,9:RGB with a linear 2% radiometric enhancement was applied on the above image. As a result, an image occurred which proved to be more suitable for lithological mapping, compared to others, for our study areas (Figure 8a). A digitization of lithological boundaries on this image, produced the map of Figure 8b.
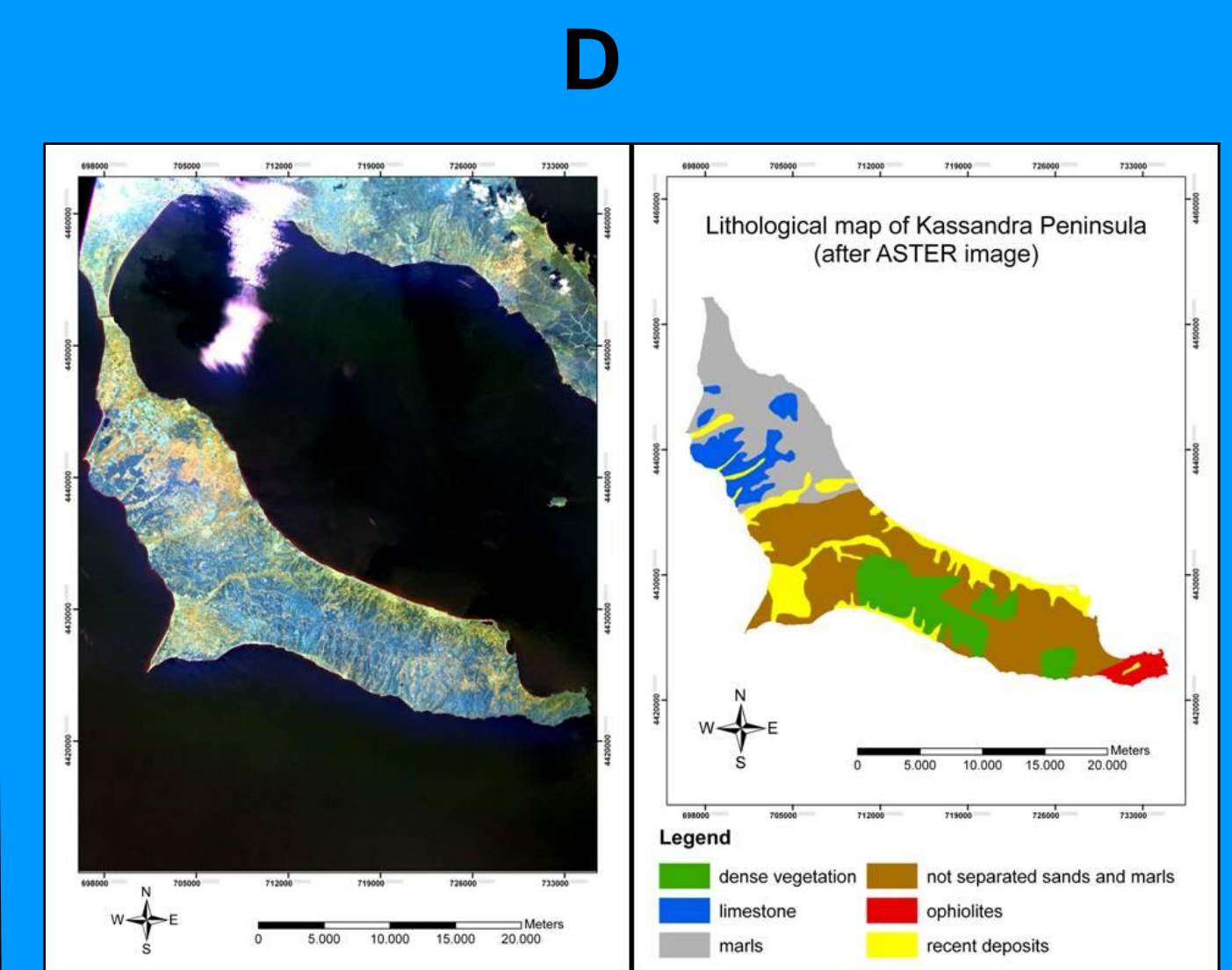

Figure 8. Kassandra peninsula: ASTER image PCA1,7,9:RGB (8a/left) and lithological map (8b/right)

4.2 TERRA/ASTER image processing/lineament mapping
Concerning lineaments, the most suitable methodology applied on the ASTER image, proved to be the 679:RGB FCC. A linear 2% enhancement was applied on the above image for improvement. After the digitization of lineaments on this image, the image-map of Figure 9a was created. The rose-diagramme of the lineaments drawn, is shown on Figure 9b.
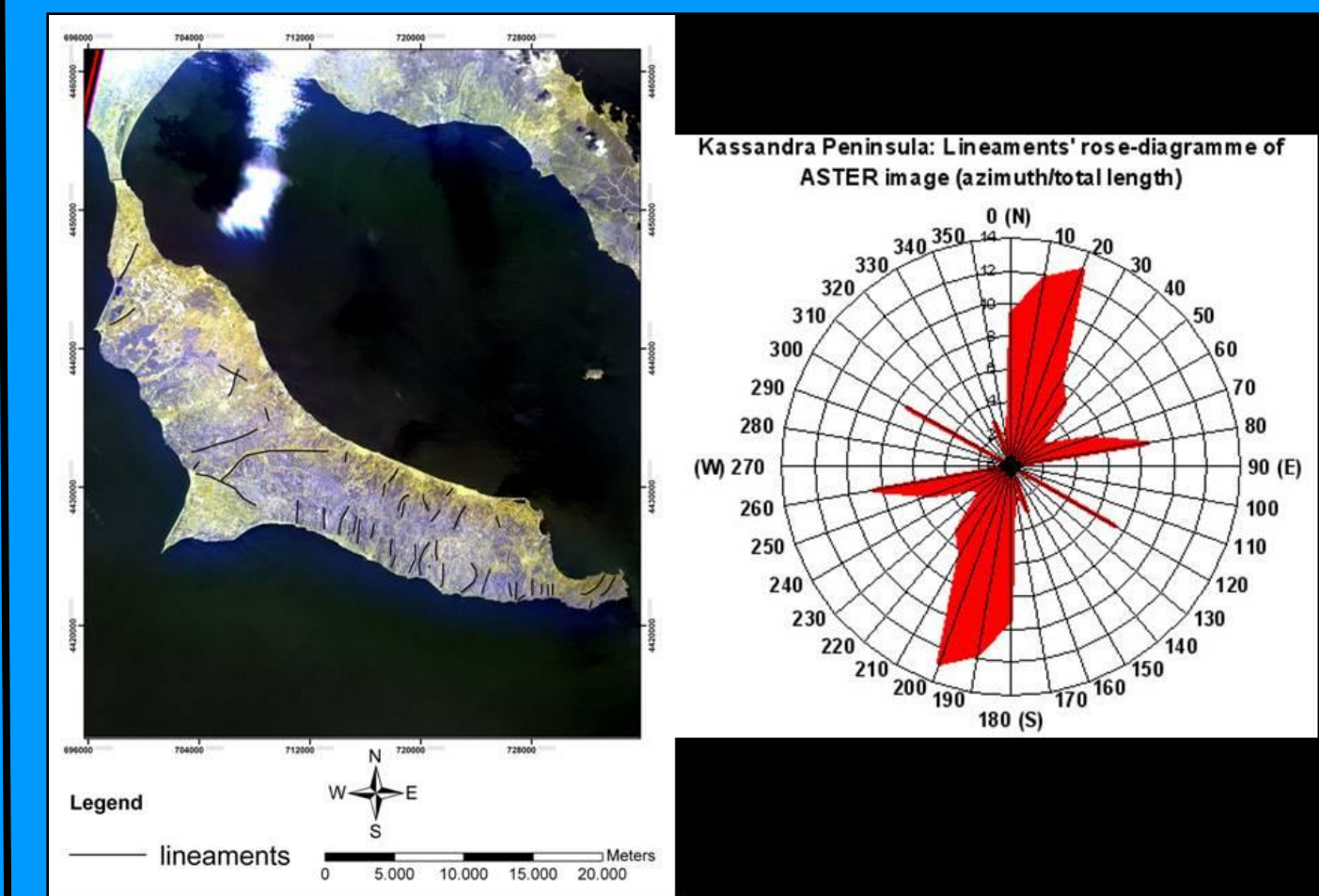

Figure 9. Lineaments of Kassandra peninsula: ASTER image 679:RGB (9a/left) and rose-diagramme (azimuth/total length per class)

5. Comparison of the derived data and results
In Kassandra peninsula, recent deposits and ophiolites were well-detected in both satellite images. Marbles were better mapped on the ASTER image than on Landsat. Marls were also well-recognized on the northern part of the Kassandra peninsula, in both images. Marls and sands could not be drawn apart in the central and southern part of the peninsula, mainly because of the dense vegetation of the area. Sandstones, conglomerates and schists could not be identified on both satellite images, because of their small coverage area.
In Thassos island, marbles, gneisses and dolomites, were mapped with satisfactory accuracy, with the exception of dense-vegetated areas. Recent deposits were delineated with relatively high accuracy. Marbles within schists were identified as gneisses most of the times. Schists within marbles and schists could not be mapped.
From the Kassandra rose-diagrammes (azimuth-length of faults per class) we see that the total lenght of lineaments in both satellite images, is higher than that of the faults of the geological map. Also, the major strike (direction) of the mapped lineaments is different than that of the faults, that is NNE-SSW, instead of NW-SE and NE-SW. There are 2 minor groups of lineaments on the satellite images that have similar strikes NW-SE and NE-SW.

From the Thassos rose-diagrammes (azimuth-length of faults per class) we see that the total length of lineaments on Landsat satellite image is higher than that of the faults of the geological map. The major strike of the mapped lineaments is significantly different than that of the faults, that is NE-SW instead of NW-SE. There is a group of faults and lineaments trending almost E-W, which was mapped in both the geological map and the Landsat-7 image and a minor group of faults that have the same strike with main group of lineaments, NE-SW.
Summarizing, **concerning discrimination of lithological units, both Landsat-7/ETM+ and TERRA/ASTER satellite images proved satisfactory,** with the exception of densely-vegetated areas or lithological units that cover relatively small areas.
In the detection of tectonic lines, significant differences and minor similarities were found between the satellite lineaments and the faults of the geological map, concerning length and strike. This is caused by the fact that not all lineaments are tectonic lines and a thorough field investigation is the next step. Nevertheless, judging from experience on earlier projects, a significant number of the mapped lineaments will prove that they correspond to faults, meaning that the geological maps need a revision in that field.

References
1. Balafoutis H., *Contribution to the study of the climate of Macedonia and Westenr Thrace (PhD Thesis in Greek)*, Thessaloniki, 1977.
2. ENVI, *ENVI 4.2 User's Guide, volumes 1 and 2*, 2005.
3. http://image2000.jrc.ec.europa.eu
4. Institute of Geological and Mineral Exploration (IGME). Geological maps sheets: Kassandra Peninsula (1970) and Thassos Island (1982). Scale 1/50.000.
5. Raharimahefa T. and Kusky T., Structural and remote sensing analysis of the Betsimisaraka Suture in northeastern Madagascar, *Gondwana Research* 15 (2009), 14-27.

→ 5th ESA EARTH OBSERVATION SUMMER SCHOOL
ON EARTH SYSTEM MONITORING & MODELLING
2-13 August 2010 | ESA-ESRIN | Frascati (Rome) Italy